Adaptive Resource Allocation for Diverse Safety Message Transmissions in Vehicular Networks

Jiayin Chen, *Member, IEEE*, Huaqing Wu, *Member, IEEE*, Feng Lyu, *Member, IEEE*, Peng Yang, *Member, IEEE*, Qihao Li, *Member, IEEE*, and Xuemin Shen, *Fellow, IEEE*

***Abstract*— In this paper, we propose a two-level adaptive resource allocation (TARA) framework to support vehicular safety message transmissions. In particular, three types of safety messages are considered in urban vehicular networks, i.e., event-triggered messages for urgent condition warnings, periodic messages for vehicular status notifications, and messages for environmental perception. Roadside units are deployed for network management, and thus messages can be transmitted through either vehicle-to-infrastructure or vehicle-to-vehicle connections. To satisfy the requirements of different message transmissions, TARA framework consists of a group-level resource reservation module and a vehicle-level resource allocation module. Particularly, the resource reservation module is designed to allocate resources to support different types of message transmissions for each vehicle group at the first level. To learn the implicit relationship between the resource demand and message transmission requests, a supervised learning model is devised in the resource reservation module, where to obtain the training data we further propose a sequential resource allocation (SRA) scheme. Based on historical network information, SRA scheme offline optimizes the allocation of sensing resources, i.e., choosing vehicles to provide perception data, and communication resources. With resources reserved for each group, the vehicle-level resource allocation module is then devised to distribute specific resources for each vehicle to satisfy the differential requirements in real-time. Extensive simulation results demonstrate the effectiveness of TARA framework in terms of the high packet delivery ratio and low latency for message transmissions, and the high quality of collective environmental perception.**

***Index Terms*— Safety message transmissions, collective perception services, two-level resource allocation, vehicular networks.**

Manuscript received 21 April 2021; revised 6 September 2021; accepted 20 October 2021. Date of publication 9 November 2021; date of current version 9 August 2022. This work was supported in part by the Research Grants from the Natural Sciences and Engineering Research Council (NSERC) of Canada; in part by the National Natural Science Foundation of China under Grant 62002389 and Grant 62001180; in part by the 111 Project under Grant B18059; in part by the Natural Science Foundation of Hunan Province, China, under Grant 2021JJ20079; and in part by the Young Talents Plan of Hunan Province of China under Grant 2021RC3004. An earlier version of this paper was presented in part at IEEE ICC 2021 [DOI: 10.1109/ICC42927.2021.9500248]. The Associate Editor for this article was Z. Xiao. *(Corresponding author: Feng Lyu.)*

Jiayin Chen is with the Department of Electrical and Computer Engineering, The University of British Columbia, Vancouver, BC V6T 1Z4, Canada (e-mail: jiayinchen@ece.ubc.ca).

Huaqing Wu is with the Department of Electrical and Computer Engineering, McMaster University, Hamilton, ON L8S 4L8, Canada (e-mail: wu482@mcmaster.ca).

Feng Lyu is with the School of Computer Science and Engineering, Central South University, Changsha, Hunan 410083, China (e-mail: fenglyu@csu.edu.cn).

Peng Yang is with the School of Electronic Information and Communications, Huazhong University of Science and Technology, Wuhan 430074, China (e-mail: yangpeng@hust.edu.cn).

Qihao Li and Xuemin Shen are with the Department of Electrical and Computer Engineering, University of Waterloo, Waterloo, ON N2L 3G1, Canada (e-mail: qihao.li@uwaterloo.ca; sshen@uwaterloo.ca).

Digital Object Identifier 10.1109/TITS.2021.3124752

I. Introduction

To ENHANCE the driving safety of connected vehicles, cooperative awareness messages (CAMs) are required to be periodically exchanged among vehicles to report their real-time driving status, e.g., ID, position, speed, and direction [2], [3]. To further improve the intelligence of autonomous vehicles, the collective perception (CP) service has been proposed by the ETSI group [4]. By provisioning CP services, vehicles can generate, send, and receive collective perception messages (CPMs) to share the perceived environmental information. Besides, if a vehicle detects an accident, event-triggered messages (i.e., decentralized environmental notification messages (DENMs)) should be generated and sent out to warn its neighboring vehicles about the accident [5].

We consider the dissemination of CAMs, CPMs, and DENMs in an urban scenario. One promising technique to enable vehicular networking is the cellular-V2X (C-V2X) communication, which can use the existing cellular infrastructure to relay the packets and achieve a centralized control [6]. Particularly, messages can be exchanged among vehicles via vehicle-to-vehicle (V2V) connections. However, due to the antenna height limitation, V2V connections can be easily blocked by obstacles, such as buildings, trucks, and buses [7], [8]. Vehicle-to-infrastructure (V2I) technologies are leveraged to deal with the non-line-of-sight (NLOS) link condition, where roadside units (RSUs) relay messages for the blocked vehicles [9], [10]. Note that, to support CP services, the generated CPMs need to be processed by the RSU before being broadcasted to vehicles. Hence, CPMs should be transmitted via V2I connections, while DENMs and CAMs can be transmitted through V2V or V2I connections.

To improve the quality of message transmission, wireless resources should be properly allocated to avoid transmission collisions, considering uplink (UL) and downlink (DL) of V2I transmissions, and V2V transmissions. Moreover, to provision CP services, not only wireless resources but also sensing resources are required. The sensing resources are allocated by choosing a subset of sensing-enabled vehicles as sensing data providers, named CP seed vehicles. The sensing coverage of the chosen vehicles can be overlapped, leading to information redundancy among the generated CPMs. Therefore, the RSU aggregates original CPMs into one integrated CPM and then broadcasts out. To evaluate the quality-of-service (QoS) for CPM transmissions, the integrated sensing coverage and accuracy are measured. In contrast, the reliability, i.e., packet delivery ratio (PDR), and delay are critical to DENM and CAM transmissions. As the resources are distributed among multiple types of message transmissions, the differentiated requirements and priorities should be considered simultaneously when making decisions on the resource allocation.

In this paper, the C-V2X based urban vehicular network is considered, where RSUs with cellular technology serve as network controllers, making resource allocation decisions for the vehicles. To guarantee the reliability and minimize the latency of event-triggered DENM transmissions and periodic CAM transmissions, wireless resource allocation decisions are made, including the V2I/V2V transmission mode selection and resource block (RB) allocation. Besides, to support CP services, both sensing and wireless resources are required for CPM generation and transmission, in which the selection of CP seed vehicles is constrained by the availability of wireless resources. Thus, the quality of CP service can be optimized via joint CP seed vehicle selection and wireless resource allocation. It is challenging to solve this multi-dimensional resource allocation problem, i.e., making the optimal decisions on the V2I/V2V transmission mode selection, RB allocation, and CP seed vehicle selection, since the decisions are intercoupled in three aspects: 1) the allocation of the sensing and wireless resources for CP services; 2) the allocation of the wireless resources for transmitting DENMs, CAMs, and CPMs; and 3) the V2V/V2I mode selection for the DENM and CAM transmissions.

Considering the vehicular dynamics in terms of network topology and message transmission requests, an adaptive resource allocation scheme is necessary. To address the aforementioned challenges, we propose a two-level adaptive resource allocation (TARA) framework for safety message transmissions, consisting of a group-level resource reservation module and a vehicle-level resource allocation module, as shown in Fig. 1. The amount of resources that required by each type of message transmission is determined by the resource reservation module. It also guarantees that the overloaded transmission requests from one type of message will not affect the others. The reservation strategy should be designed to optimize the overall QoS satisfaction for all the types of message transmissions. Based on the reserved resources for different types of messages, the resource allocation module is devised to satisfy each vehicle's individual QoS requirements. The main contributions are summarized as follows:

1) *Multi-dimensional resource management* – We study the joint management of multi-dimensional resources to support safety message transmissions, which is of significant importance for future vehicular networks. By analyzing the impact of message transmission priorities and network conditions (e.g., resource availability and link reliability), wireless resources and sensing resources can be jointly allocated by the proposed TARA framework to satisfy the differential QoS requirements, the process of which is shown in Fig. 1;

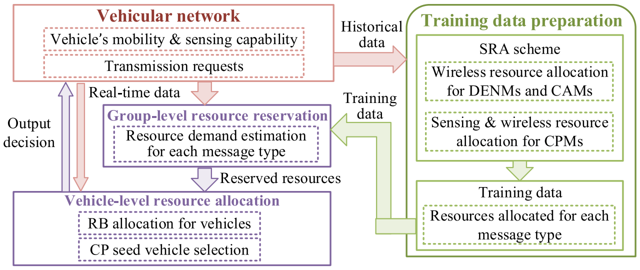

Fig. 1. Illustration of TARA framework.

2) *Sequential resource allocation (SRA) scheme* – Based on the historical information, the allocation decisions of wireless and sensing resources can be made by SRA scheme according to the transmission priority of different messages. Particularly, for DENM and CAM transmissions, vehicles are sorted by their potential gains obtained by V2I transmission, to guide the selection of V2I/V2V mode and RB allocation. For CPM transmissions, the CP seed vehicles are selected iteratively, based on vehicles' sensing performance;
3) *Enabling efficient decisions in real-time* – Since SRA scheme needs to sequentially make decisions based on message transmission priorities, it is unable to keep pace with the dynamic vehicular environment. Thus, we propose TARA framework to achieve real-time decision-making, consisting of a group-level resource reservation module and a vehicle-level resource allocation module. The resource reservation module reserves the resources to support different types of message transmissions for each vehicle group, i.e., a set of neighboring vehicles, which allows the resource allocation module to perform in parallel for different groups and different message types. The supervised learning-based technique is applied in the resource reservation module to learn the implicit relation between the resource demand and message transmission requests, which is offline trained based on the data provided by SRA scheme. With the reservation result, resources are allocated to each vehicle by the vehicle-level resource allocation module, which can be achieved in real-time with a low time complexity.

The remainder of this paper is organized as follows. We review the related work in Section II, and describe the system model in Section III. We give an overview of the developed TARA framework in Section IV. SRA scheme is devised in Section V. To further improve the time efficiency of resource allocation, a group-level resource reservation module and a vehicle-level resource allocation module are designed in Section VI. Simulation results are carried out in Section VII to demonstrate the performance of the proposed framework. Finally, conclusion and future work are drawn in Section VIII.

II. Related Work

A. Reliable Safety Message Dissemination

To support the periodic safety message dissemination, a mobility-aware time division multiple address medium

TABLE I
COMPARISON OF RELATED WORKS WITH THE PROPOSED WORK

	Reference	Supported services	Management parameters
Safety message dissemination	[11]	periodic message transmission	time slot assignment
	[12]	periodic message transmission	MAC protocol design
	[13]	periodic and event-triggered message transmission	message length
	[14]	periodic and event-triggered message transmission	beacon rate
	[15]	message transmission in urban scenario	RSU deployment
Resource allocation	[19]	content downloading	content caching and delivery
	[20]	rate constrained and delay constrained services	group-level resource reservation
	[21]	URLLC and eMBB services	group-level resource reservation
	[22]	CAM transmission	resource block size for V2V connection
	[23, 24]	CAM transmission	vehicle-level resource allocation for V2V
	[25]	CAM transmission	vehicle-level resource allocation for V2I and V2V
Proposed scheme	TARA	CAM, DENM, and CPM transmissions	vehicle-level resource allocation and group-level resource reservation for V2I and V2V

TABLE II
COMPARISON OF THREE TYPES OF SAFETY MESSAGES [2], [4], [5]

Message type	Generation interval	Priority	Requirement	Transmission mode
DENM	Event-triggered	High	High reliability, low latency	V2V / V2I
CAM	Periodic (fixed CAM period, e.g., 100 ms)	Medium	High reliability, low latency	V2V / V2I
CPM	Periodic (adjustable CPM period)	Low	Sensing coverage and accuracy	V2I

access control (MAC) protocol was proposed in [11] to avoid slot-assignment collisions, where vehicles on different lanes of road segments are assigned with disjoint time slot sets. Furthermore, a hybrid MAC protocol, which is partially centralized and partially distributed, was developed to improve the PDR and normalized throughput [12]. In addition to periodic messages, e.g., the beacon message and the map data message [13], event-triggered safety messages are generated and transmitted by vehicles as well, which is essential for cooperative driving among vehicles. In [14], the beacon rate was optimized to meet the reliability requirements of event-triggered safety messages and maintain the accuracy of neighborhood information collected by beacons. In urban intersection scenarios, RSUs deployed at intersections have been widely leveraged to enhance the packet transmission [15], [16], where V2I connections are implemented to complement V2V connections among vehicles.

B. Adaptive Resource Allocation for Vehicular Networks

To support diversified vehicular applications, slicing schemes are developed to reserve resources for various services [17], [18]. In [19], a service-dependent resource slicing scheme was developed to satisfy the differentiated requirements of content downloading services, through making decisions on the RSU transmission rate and content caching. In [20], resource slicing was adopted to establish slices for two sets of applications, the rate constrained and the delay constrained applications, and resources allocated to each individual slice were adapted to the user population. An online network slicing strategy was developed in [21], aiming to maximize the long-term time-averaged system capacity while satisfying the strict requirements of ultra-reliable low-latency communication (URLLC) and enhanced mobile broadband (eMBB) services.

To further allocate the required resources to each vehicle, C-V2X mode-3 resource scheduling schemes are investigated for V2V connections [22]. In [23], vehicles were grouped into non-overlapping clusters, then the mode-3 resource scheduling was designed for each cluster to perform sub-channel assignment. Not only the prevention of allocation conflicts but also the fulfillment of QoS should be considered when allocating sub-channels to the vehicles [24]. To deal with the NLOS issue, an RSU relaying system named relay assisted enhanced V2V was proposed in [25], where the RSU and vehicular users operate on the same frequency band during the assigned separate time slots. Specifically, the distributed decisions on resource scheduling and the V2I/V2V resource separate ratio are made by vehicles and the RSU, respectively.

C. Discussion

In spite of the aforementioned works as summarized in Table I, the following issues are insufficiently studied in literatures, while are essential for resource allocation in RSU assisted vehicular networks.

1) In existing works, vehicular services are divided into different types, e.g., safety-related and non-safety services. However, the safety-related services can present different traffic patterns and service requirements, as given in Table II, which is rarely considered;
2) Resource allocation schemes with different levels, which were studied separately in most existing works, are jointly investigated in this work. Through joint optimization of the group-level resource reservation and the vehicle-level resource allocation, the overall performance can be further improved. For instance, the vehicle-level resource allocation can provide feedback about resource utilization and QoS satisfaction for adaptive resource reservation in real time;

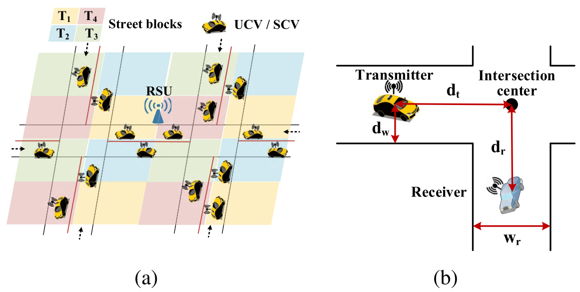

Fig. 2. Illustration of: a) vehicular network; b) NLOS case.

3) Safety messages are transmitted via V2V or V2I connections on the same frequency band, which calls for a resource allocation scheme considering V2I and V2V mode selections. However, most of the existing resource reservation/slicing schemes only consider V2I links, while most of the vehicle-level resource allocation schemes are developed for V2V links. To bridge the gap, TARA framework is proposed in this paper, considering both V2V and V2I transmissions and specific performance metrics of multifarious types of messages.

III. System Model

A. Network Model

As shown in Fig. 2(a), we consider a vehicular network in the urban scenario, including connected vehicles (CVs) and RSUs. According to the capability of sensing, the vehicles are classified into two types, namely the sensing-enabled CVs (SCVs) and CVs without sensing capability (UCVs). With vehicular sensors, an SCV can observe the environment within its sensing range and generate the sensing report, which includes the information of detected objects. The RSU can not only relay the packets, but also make resource allocation decisions for vehicles. A network management controller is deployed at the RSU, to collect the information (e.g., the vehicle's location, request, and sensing reports) and make decisions accordingly. Without loss of generality, we focus on the coverage area of one RSU. In our work, vehicles are clustered as non-overlapped groups. As shown in Fig. 2(a), vehicles in one square block constitute a group. For the sake of simplicity, we assume the block's side length equals the V2V communication range, hence there is no V2V connection between vehicles within any two nonadjacent blocks. Important mathematical symbols are listed in Table III. In this paper, the subscripts i, j, m, and R represent the i-th time segment, the j-th vehicle group, the m-th sub-frame, and the RSU, respectively. The superscripts A, D, P, PU, PD, and m represent the CAM, DENM, CPM, CPM uploading, CPM downloading, and the m-th vehicle, respectively.

1) Communication Model: The path loss between two vehicles are modeled separately in line-of-sight (LOS) [26] and NLOS [8] cases, respectively. For LOS cases, the path loss is

$$PL_L(x) = 20\log_{10}(\frac{4\pi x}{\lambda}) \tag{1}$$

where x is the distance between receiving and transmitting vehicles and λ is wavelength of transmission frequency. As shown in Fig. 2(b), the path loss for NLOS cases is

$$PL_N(d_t, d_r, d_w) = 3.75 + \begin{cases} 10\log_{10}\left(\left(\frac{d_t^{0.957}}{(d_w w_r)^{0.81}}\frac{4\pi d_r}{\lambda}\right)^{n_{NLOS}}\right), & \text{if } d_r \le d_b, \\ 10\log_{10}\left(\left(\frac{d_t^{0.957}}{(d_w w_r)^{0.81}}\frac{4\pi d_r^2}{\lambda d_b}\right)^{n_{NLOS}}\right), & \text{if } d_r > d_b \end{cases} \tag{2}$$

where d_t (and d_r) is the distance between the transmitting (and receiving) vehicle and the intersection-center, d_w is the distance between the transmitting vehicle and the road-side, w_r is the width of the receiving street, d_b is a reference parameter called critical distance, and n_{NLOS} is the NLOS path loss exponent. Note that, the path loss model for NLOS cases can be applied to intersections with different corner angles, in addition to the 90-degree corner [27], [28].

The receiving signal power P_{RX} (dBm) is obtained based on the transmit power P_{TX} (dBm), path loss, and receiver's antenna gain G_r (dB),

$$P_{RX} = P_{TX} + G_r - \begin{cases} PL_L(x), & \text{LOS}, \\ PL_N(d_t, d_r, d_w), & \text{NLOS}. \end{cases} \tag{3}$$

The message can be successfully decoded when P_{RX} is larger than the threshold of decoding received signal strength.

2) Half-Duplex Problem of Connected Vehicles: The target receiver set for each transmitting vehicle consists of vehicles within the targeting message dissemination range, which is set as the V2V communication range in our work. Taking into account the half-duplex feature of CVs, they are not capable of receiving and transmitting packets simultaneously. In our work, time is partitioned into sub-frames with constant duration, which is applied as the unit of time in resource allocation. If a sub-frame is allocated for a source vehicle to transmit its packets through V2V connections, this sub-frame should not be reused by the target receivers for packet transmitting (V2V or V2I UL transmission). Hence, as shown in Fig. 2(a), to deal with the half-duplex issue, the adjacent four vehicle groups are allocated with isolated time segments (T_i, $i = 1, \ldots, 4$). Each time segment T_i consists of t_i sub-frames. Although vehicles in nonadjacent blocks are allocated with the same time segment, there is no interference among them due to spatial separation since the side length of each street block is set to be V2V communication range.

B. Wireless Resource Pool

In this work, the V2V, V2I UL, and V2I DL transmissions are assumed to share a frequency band of 10 MHz (from 5.89 to 5.9 GHz), which is divided into 50 sub-channels. For the time domain, one sub-frame is defined as the duration of 1 ms [29]. As shown in Fig. 3, the wireless resource pool of T_i segment is represented by the combination of $50 \cdot t_i$ RBs, each of which represents the usage of 200 kHz bandwidth for 1 ms. Hence, the wireless resource allocation can be performed via allocating RBs to vehicles for packet transmissions. The numbers of required RBs for DENM, CAM,

TABLE III
SUMMARY OF MATHEMATICAL SYMBOLS

Symbols	Definition	Symbols	Definition
$A_{i,j,m}$	Number of unoccupied RBs in $S_{i,m}$ available for CPM transmitted by $V_{i,j}$	$C_{i,j}^P$ (C_R^P)	Number of supported CPM uploading for group $V_{i,j}$ (the RSU)
$B_{i,m}$	Number of groups contending $S_{i,m}$ for CPM	C	Threshold of sensing coverage
D_a (D_r)	Available (Required) RB number for V2I DL	d	Distance from sensing block center to SCV
d_b	Critical distance of NLOS model	d_w	Distance from the transmitter to the road-side
d_t (d_r)	Distance between the transmitting (receiving) vehicle and the intersection-center	e (e_0)	SCV's sensing error for a given block (Penalty error for not sensed blocks)
G_i	Number of vehicle groups with segment T_i	$G_{i,j}^m$	Potential packet loss under V2V mode of $V_{i,j}^m$
G_r	Receiver's antenna gain (dB)	$I_{i,j}$ ($D_{i,j}$)	Number of TDSs (packets transmitted in TDSs) in $V_{i,j}$
$M_{i,j}^m$ ($S_{i,j}^m$)	Number of vehicles in the target (successful) receiver set of $V_{i,j}^m$	$N_{i,j}^D$ ($N_{i,j}^A$)	Number of V2I UL RBs allocated to the vehicles requesting for DENM (CAM)
n_{NLOS}	NLOS path loss exponent	PL_L (PL_N)	Path loss of the LOS (NLOS) case (dB)
P_{RX} (P_{TX})	Receiving (transmitting) signal power (dBm)	R	Sensing range of vehicular sensor
$R_{i,j}$ ($R_{i,j}^P$)	Overall number of DENM and CAM (Number of CPM) requests raised by $V_{i,j}$	S^D (S^A, S^{PU}, S^{PD})	The numbers of required RBs for DENM (CAM, CPM upload, CPM download)
$S_{i,m}$	The m-th sub-frame in time segment T_i	T_i (T_i^n)	The i-th time segment (Segment i of n-th CAM period)
t_i	Number of sub-frames in time segment T_i	T^P ($T_{i,j}^P$, T_R^P)	CPM period (Required CPM period of $V_{i,j}$ or RSU)
$V_{i,j}$ ($V_{i,j}^m$)	The j-th vehicle group with time segment T_i (The m-th vehicle in $V_{i,j}$)	V_S (V_S^+)	Sorted set of vehicles with message requests (Subset of V^S with positive $G_{i,j}^m$)
V^D (V^{D+}, V^{D0})	Set of vehicles with DENM requests (Subset of V^D with positive or zero $G_{i,j}^m$)	V^A (V^{A+}, V^{A0})	Set of vehicles with CAM requests (Subset of V^A with positive or zero $G_{i,j}^m$)
$V_{i,j}^U$	Set of messages not under V2I mode in $V_{i,j}$	w_d (w_t)	Unit sensing error of distance (CPM update delay)
w_r	Width of the receiving street	X	Number of V2I packets can be transmitted in one TDS
x	Distance from receiver to transmitter	λ	Wavelength of transmission frequency
ρ_i	The frequency partition ratio for segment T_i		

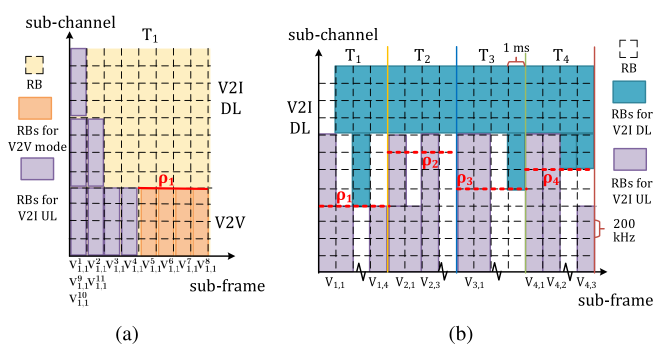

Fig. 3. An illustration of resource allocation: a) within one vehicle group; b) for V2I connections within the RSU.

CPM uploading (packet transmission from SCVs to the RSU), and CPM downloading (the integrated packet transmission from the RSU to vehicles) are denoted by S^D, S^A, S^{PU}, and S^{PD}, respectively. As shown in Fig. 3, in order to prevent the packet reception collisions, a ratio is defined to partition the frequency band between V2I DL and V2V transmissions, denoted by ρ_i ($i = 1, \ldots, 4$) for the vehicle group with time segment T_i. Specifically, if one sub-frame is allocated for V2V transmission in segment T_i, the first $50 \cdot \rho_i$ sub-channels are available for V2V, while the remaining sub-channels are available for V2I DL transmissions. Otherwise, the 50 sub-channels are available for V2I DL transmissions as long as they are not occupied by V2I UL.

There are G_i vehicle groups being allocated with the same time segment, T_i, and the j-th group of which is denoted by $V_{i,j}$, consisting of $K_{i,j}$ vehicles, as shown in Fig. 3. The m-th vehicle in $V_{i,j}$ is denoted by $V_{i,j}^m$, $m = 1, \ldots, K_{i,j}$. To deal with the half-duplex problem and avoid the packet transmission collisions, the following principles should be followed by the wireless resource allocation for vehicles:

1) *V2V and V2I UL for each vehicle group* – Considering the half-duplex feature, separate sub-frames are allocated to vehicles transmitting packets via V2V connections. The number of sub-frames required by one vehicle can be calculated based on ρ_i and the size of the packet. In our work, ρ_i is determined to ensure that each V2V transmission can be finished by one sub-frame. For a vehicle group, in addition to the sub-frames assigned for V2V transmissions, the unoccupied sub-frames can be allocated for V2I UL transmissions. In Fig. 3(a), the wireless resource allocation for both V2V and V2I UL transmissions in the vehicle group $V_{1,1}$ is illustrated as an example, where multiple vehicles can use the distinct RBs in the same sub-frame for V2I UL transmissions;
2) *V2I UL for vehicle groups with the same time segment* – Within the coverage of one RSU, all the vehicles under V2I mode transmit their packets to the RSU. Thus, V2I UL collision may happen among the G_i vehicle groups with the same time segment, T_i. To avoid the collision, these G_i groups should be considered simultaneously when making resource allocation decisions on V2I UL transmissions. As shown in Fig. 3(b), for the vehicles from $V_{i,j}$, $j = 1, 2, \ldots, G_i$, the V2I RBs allocated to them shall not overlap with each other;
3) *V2I DL for vehicles under the RSU* – V2I DL RBs are required for relaying the packets transmitted via

V2I mode, such as the DENM, CAM, and integrated CPM packets. Since the V2I DL and V2V transmissions are assigned with separate frequency bands, there is no interference among them. When making V2I DL RB allocation decisions, only the V2I UL transmissions are considered to avoid potential collisions. In each time segment, the RBs beyond the V2V frequency bound are available for V2I DL transmission, as long as they are not allocated for V2I UL transmissions. The V2I DL resource pool consists of the available RBs from the four time segments, which is shared by all the vehicles within the RSU coverage, as shown in Fig. 3(b). For one V2I mode packet, its assigned sub-frames for DL transmission have to be after that for UL.

C. QoS for Safety Message Transmissions

To evaluate the performance of message transmissions, we consider differentiated metrics for multifarious messages:

1) *DENM and CAM* – Both latency and reliability are critical to DENM and CAM transmissions. The transmission delay of one packet is measured as the time elapsed between it being transmitted and received. For the reliability, the PDR is measured;
2) *CPM* – The performance of CPM transmission is evaluated by the quality of CP services. For one SCV, its sensing coverage area is a circular disk, the radius of which is the sensing range R. Within the sensing range, objects can be detected, but the sensing accuracy degrades with the distance between the object and the SCV. Given the set of CP seed vehicles, the integrated sensing accuracy can be calculated by the RSU according to the contents, transmission latency, and update frequency of CPMs. On the other hand, the coverage rate, i.e., the proportion of the perceived street area to the overall street area, is also evaluated as one performance metric of CP services. Given a threshold of the coverage rate, the selection of CP seed vehicles and wireless resource allocation are performed to guarantee the coverage rate and achieve the optimal integrated sensing accuracy.

IV. Overview of TARA Framework

In this work, the requests of the DENM and/or CAM transmission are sent by vehicles, and then the RSU allocates a specific bunch of RBs accordingly. To support CP services, the decisions on both sensing and wireless resource allocation are also made by the RSU. We propose TARA framework, including a group-level resource reservation module and a vehicle-level resource allocation module, to make resource allocation decisions. In addition, data preparation is also needed to train the learning-based resource reservation model offline, as shown in Fig. 1.

A. Training Data Preparation

To prepare training data for the learning-based resource reservation model, we propose SRA scheme to achieve optimal

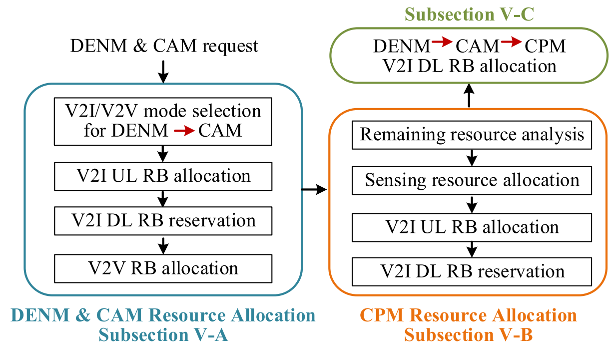

Fig. 4. Sequential resource allocation procedures.

resource allocation decisions, based on the historical information on vehicle's mobility, e.g., location and speed, sensing capability, and transmission requests. To support CP services and transmissions of DENMs and CAMs, decisions are made for sensing and wireless resources, including the RBs allocated for vehicles and the selected CP seed vehicle set. With the proposed SRA scheme, the number of RBs allocated to each message type can be obtained as training data, which indicates the underlying mapping relationship between the allocated resources and message transmission requests.

The procedure of SRA scheme is shown in Fig. 4. Considering the differential priorities of message transmissions, SRA scheme is devised to allocate the resources for the DENM and CAM firstly, followed by the CPM resource allocation procedures. Recall that V2I DL resource pool is determined by the V2I UL resource allocation results and the frequency partition ratio ρ_i. Therefore, the V2I DL RBs are allocated after performing V2I UL RB allocation procedures. Considering the wireless resources required to transmit one packet, both V2I UL and DL resources should be allocated for the V2I mode, which is double of the resources required by the V2V mode. Therefore, to make efficient resource allocation decisions, the V2I mode is selected for one transmission only when the V2V mode cannot meet its requirement. In terms of the V2I mode selection for DENM and CAM transmissions, the vehicle with a stronger demand on the V2I resources has a higher priority. Meanwhile, to support CP services, wireless and sensing resources are allocated through: 1) analyzing the CPM uploading capacity available for each vehicle group based on the RB allocation results of DENM and CAM; and 2) greedily selecting the CP seed vehicles based on their sensing gains. Details of SRA scheme are given in Section V.

B. Resource Reservation and Resource Allocation Modules

Based on the decisions made by SRA scheme, we can obtain the number of RBs allocated for message transmissions. In light of the relationship between the number of allocated RBs and message transmission requests, we leverage the two-level resource management strategy to enable a parallel decision-making for vehicles requesting different messages. To make real-time decisions for different types of requests, we design the group-level resource reservation module and the vehicle-level resource allocation module, as shown in

Fig. 1 and elaborated in Section VI. The learning-based resource reservation model is trained based on the wireless resource allocation results achieved by SRA scheme. Based on the network information, the resource reservation module distributes resources to support the transmission of different types of messages for each group. With the reserved resources, RBs are allocated to each vehicle by the resource allocation module. In addition, the selection of CP seed vehicles and required RBs for CPM transmissions are also determined by the resource allocation module.

V. Design of SRA

In this section, we present the designed SRA scheme to achieve the optimal resource allocation result, part of which is presented in our previous work [1]. In this work, to adapt to environmental dynamics in terms of the vehicle mobility and event-triggered DENM requests, the resource allocation decisions are updated every CAM period, i.e., 100 ms [2]. One CAM period is divided into four time segments, each of which consists of 25 sub-frames, i.e., $t_i = 25$ for $i = 1, \ldots, 4$.

A. Resource Allocation for DENM and CAM Transmissions

At each CAM period, the RSU allocates wireless resources for vehicles requesting DENM and CAM transmissions, which are denoted by two sets V^D and V^A, respectively. Firstly, the RSU collects the vehicles' location information and obtains the target receiver set for each vehicle $V^m_{i,j}$. Considering the potential NLOS link conditions between $V^m_{i,j}$ and its $M^m_{i,j}$ target receivers, the number of vehicles that can successfully receive the packet via V2V connections is denoted by $S^m_{i,j}$, where $S^m_{i,j} \leq M^m_{i,j}$. For each transmission, the V2I mode is selected only when any of the following events happen:

1) *Sub-frame insufficiency* – Within one vehicle group $V_{i,j}$, the V2V transmissions request separate sub-frames to avoid the collision. In the case of pure V2V mode, i.e., all vehicles transmit packets via V2V connections, at least $R_{i,j}$ sub-frames are required, where $R_{i,j}$ denotes the overall number of DENM and CAM requests raised by $V_{i,j}$. If $R_{i,j} > t_i$, the sub-frames are insufficient for $V_{i,j}$ in the pure V2V mode. Recall that multiple packets can be transmitted in one sub-frame under the V2I mode. The sub-frame insufficiency issue can be mitigated through selecting the V2I mode for specific packet transmissions;
2) *NLOS condition* – If the NLOS link condition encounters between transmitting and receiving vehicles, the V2V connection based packet transmission may be blocked. To improve the reliability, the NLOS affected packets should be relayed by the RSU via V2I connections. For each transmitting vehicle $V^m_{i,j}$, its potential packet loss under the V2V mode can be estimated by the RSU, denoted by $G^m_{i,j} = M^m_{i,j} - S^m_{i,j}$. As the packet loss can be avoided via selecting the V2I mode, $G^m_{i,j}$ is defined as the potential V2I selecting gain for $V^m_{i,j}$, a larger value of which indicates a higher priority of utilizing V2I resources.

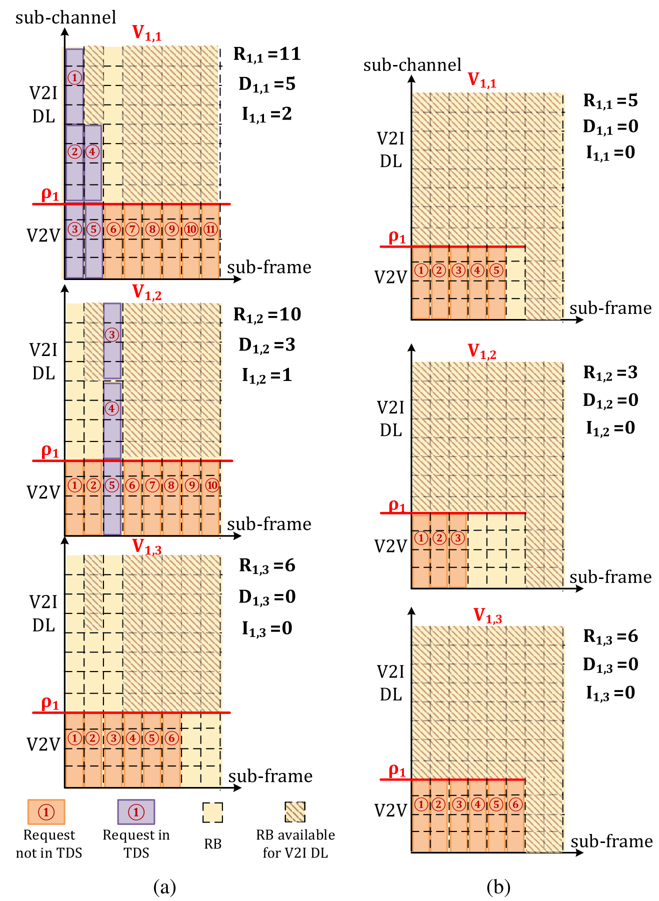

Fig. 5. An illustration of resource allocation: a) insufficient sub-frame case; b) sufficient sub-frame case.

The resource allocation can be operated by following steps:

1) *Determine vehicles' priorities* – Considering the street layout and the receiving signal power calculated based on Eq. (3), the value of $G^m_{i,j}$ can be obtained for each vehicle in V^D and V^A. The set of vehicles requesting DENM (CAM) transmissions with positive $G^m_{i,j}$, i.e., packet loss will occur if the vehicle is assigned with the V2V mode, is denoted by V^{D+} (V^{A+}), in which the vehicles are sorted in descending order by $G^m_{i,j}$. Likewise, the sets of vehicles with $G^m_{i,j} = 0$ are denoted by V^{D0} and V^{A0}, respectively. Due to the higher priority of DENM requests, the sorted set is recombined as $V_S = \left\{V^{D+}, V^{A+}, V^{D0}, V^{A0}\right\}$, and its subset consisting of vehicles with positive gain is defined by $V^+_S = \left\{V^{D+}, V^{A+}\right\}$. When assigning the V2I mode for vehicles, the vehicles' priorities are indicated by their orders in V_S or V^+_S;
2) *Calculate the required number of transmitting dominant sub-frames* – For each sub-frame, the RBs can be allocated for V2V, V2I UL, and V2I DL transmissions, in which the RBs for V2V and V2I UL transmissions always occupy lower frequency band as shown in Fig. 3. To reserve more RBs for V2I DL transmissions, the V2I UL should occupy the RBs within the V2V frequency band, unless the group $V_{i,j}$ suffers from the sub-frame

insufficiency. If the proportion of transmitting RBs is larger than ρ_i, the sub-frame is defined as a transmitting dominant sub-frame (TDS). An example of resource allocation for T_1 segment is illustrated in Fig. 5, where $G_1 = 3$ and $t_1 = 8$. Since $R_{1,1}\left(R_{1,2}\right) > t_1$ in the case given in Fig. 5(a), the sub-frames are insufficient for $V_{1,1}$ and $V_{1,2}$ under the pure V2V mode. Thus, 5 and 3 requests are required to be transmitted in TDSs for $V_{1,1}$ and $V_{1,2}$, respectively. For vehicle group $V_{i,j}$, since one TDS can be shared by at most X $(X > 0)$ V2I UL transmissions, the required number of TDSs $(I_{i,j})$ and the number of requests transmitted in TDSs $(D_{i,j})$ can be calculated by

$$I_{i,j} = \left\lceil \max\left(R_{i,j} - t_i, 0\right) / (X - 1) \right\rceil, \tag{4}$$

$$D_{i,j} = \max\left(R_{i,j} - t_i + I_{i,j}, 0\right). \tag{5}$$

Hence, the RSU assigns the V2I mode for $D_{i,j}$ transmission requests in $V_{i,j}$, according to their priorities, i.e., the orders in V_S. Then, the set of transmissions not assigned with V2I mode is denoted by $V_{i,j}^U$;

3) *Assign sub-frames for packet transmission* – In segment T_i, the first $I_{i,1}$ sub-frames are allocated to $V_{i,1}$ as its TDSs, the following $I_{i,2}$ sub-frames are allocated as the TDSs for $V_{i,2}$, and so forth. In $V_{i,j}$, these $I_{i,j}$ TDSs are assigned for the $D_{i,j}$ transmissions in the V2I mode. For the remaining transmissions in $V_{i,j}^U$, each is assigned with one specific sub-frame, always starting by occupying the first available sub-frame in T_i. Two examples of sub-frame assignment for the three groups in segment T_1 are illustrated in Fig. 5(a) and Fig. 5(b), considering the cases of sufficient and insufficient sub-frame, respectively;

4) *Determine the available RB pool for V2I DL transmissions* – Based on the sub-frame assignment, the number of available RBs for V2I DL transmission is determined, denoted by D_a. The available V2I DL RBs for T_1 segment are displayed in Fig. 5. Notice that, the RBs below the V2V frequency band can be used by V2I DL transmission only in the sub-frames unoccupied by any groups in the segment, as the last two sub-frames shown in Fig. 5(b). Meanwhile, for the transmissions already assigned with V2I modes, the overall number of required V2I DL RBs can be obtained as well, denoted by D_r;

5) *Select V2I modes for NLOS condition* – Since the V2I UL RBs in segment T_i are shared by G_i groups, the requests in $V_{i,j}^U$, $j = 1, \ldots, G_i$, with positive $G_{i,j}^m$ are jointly considered and assigned with V2I modes based on their orders in V_S^+ until the resources are depleted, i.e., $D_r \geq D_a$. In each iteration, the required V2I UL RBs are allocated to the selected transmission in its assigned sub-frame, if the RBs are not allocated for V2I UL transmission yet. Otherwise, this transmission will be assigned with a new sub-frame unoccupied by V2I UL. At the end of each iteration, the $V_{i,j}^U$, D_a, and D_r are updated accordingly;

Algorithm 1 RB Allocation Adjustment to Minimize T^P

1 **Input:** Initial RB allocation results for DENM and CAM transmissions; number of CPM transmission requests, $R_{i,j}^P$;
2 **Output:** Modified RB allocation for DENM and CAM transmissions; required CPM period, T^P; $C_{i,j}^P$ and C_R^P;
3 Calculate $C_{i,j}^P$, C_R^P, $T_{i,j}^P$, and T_R^P;
4 The candidate group for adjustment, $\mathbb{C} = \left\{V_{i,j} | T_{i,j}^P > T_R^P\right\}$;
5 **while** $\mathbb{C}$ *is not empty* **do**
6   Find the group with the largest $T_{i,j}^P$ in $\mathbb{C}$, $V_{i,j}$;
7   **for** *The sub-frame assigned for V2V transmission in* $V_{i,j}$, $S_{i,m}$ **do**
8   Assuming $S_{i,m}$ is modified to V2I mode for $V_{i,j}$, calculate the potential $C_{i,j}^P$, $j = 1, \ldots, G_i$, and C_R^P;
9   **if** *Existing* $C_{i,j}^P$ *or* C_R^P *becomes 0* **then**
10   Do not modify the transmission mode of $S_{i,m}$;
11   **else**
12   Modify the transmission mode of $S_{i,m}$ to V2I;
13   Update $B_{i,m}$, D_r, $C_{i,j}^P$, and C_R^P;
14   Update $T_{i,j}^P$, T_R^P, and $\mathbb{C}$;
15   **if** $V_{i,j}$ *is not the group with the largest* $T_{i,j}^P$ *in* $\mathbb{C}$ **then**
16   Terminate the modification for $V_{i,j}$;
17   Turn to Line 6;
18   Remove $V_{i,j}$ from $\mathbb{C}$;
19 Calculate the required CPM period, $T^P = \max(T_{i,j}^P, T_R^P)$.

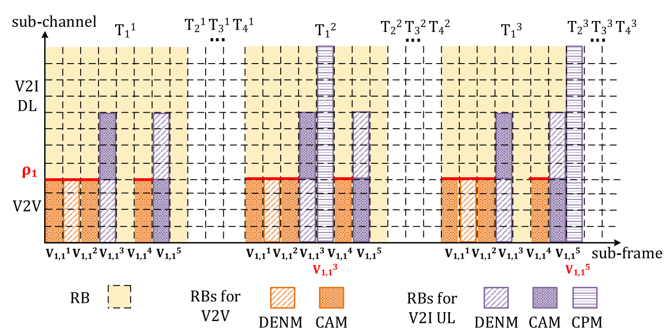

Fig. 6. An illustration of resource allocation for DENM, CAM, and CPM.

6) *Allocate V2V RBs* – The V2V mode is selected for each transmission in $V_{i,j}^U$, and the required V2V RBs are allocated in its assigned sub-frame.

B. Resource Allocation for CPM Transmissions

1) Wireless Resource Allocation: Given the resource allocation result for DENM and CAM transmissions during each CAM period, the number of supported CPM uploading for group $V_{i,j}$ and the RSU, denoted by $C_{i,j}^P$ and C_R^P, respectively, can be obtained as follows. Recall that CPM packets need to be uploaded via V2I connections.

- *Contending degree of sub-frames* – For each group $V_{i,j}$, the sub-frames unallocated for V2V transmission can be used for CPM upload. Hence, the unoccupied RBs in a non-V2V sub-frame can be potentially allocated for CPM uploading, which may be contended by multiple vehicle groups with the same segment. For the m-th sub-frame in T_i segment, $S_{i,m}, m = 1, \ldots, t_i$, the number of groups that contend $S_{i,m}$ for CPM uploading is defined as the contending degree of sub-frame $S_{i,m}$, denoted by $B_{i,m}$;

- *Supported CPM uploading for each group* – For group $V_{i,j}$, if sub-frame $S_{i,m}$ is not allocated for the V2V transmission, the unoccupied RBs in $S_{i,m}$ are available for CPM uploading, the number of which is denoted by $A_{i,j,m}$. The $C^P_{i,j}$ is calculated as the weighted summation of $A_{i,j,m}$, i.e., $C^P_{i,j} = \left\lfloor \left(\sum_{m=1}^{t_i} A_{i,j,m}/B_{i,m}\right) / S^{PU} \right\rfloor$;
- *Supported CPM uploading for RSU* – Besides the limitation of $C^P_{i,j}$, the RB reservation for V2I DL transmissions should be considered as well. Thus, the overall available number of RBs for CPM uploading under the RSU coverage is determined by the gap between the available and required numbers of V2I DL RBs, i.e., $C^P_R = \left\lfloor \left(D_a - D_r - S^{PD}\right) / S^{PU} \right\rfloor$. Notice that, D_r represents the required number of V2I DL RBs for the DENMs and CAMs, while S^{PD} represents that for the integrated CPM packet.

Given the number of CPM requests for each group $V_{i,j}$, denoted by $R^P_{i,j}$, the required CPM uploading interval (named by CPM period) is designed as an integral multiple of the CAM period. The integral multiplier, T^P, is calculated by

$$T^P = \max(T^P_{i,j}, T^P_R) = \max\left(\left\lceil R^P_{i,j}/C^P_{i,j} \right\rceil, \left\lceil \left(\textstyle\sum_i \sum_j R^P_{i,j}\right)/C^P_R \right\rceil\right) \tag{6}$$

where the required CPM period for each group and RSU are denoted by $T^P_{i,j}$ and T^P_R, respectively. Since a longer CPM uploading delay results in a larger sensing error, T^P should be minimized via improving the C^P_R and $C^P_{i,j}$. However, the C^P_R can be improved only through modifying the selected V2I mode to V2V mode, which may lead to the packet loss of DENMs and CAMs. On the contrary, $C^P_{i,j}$ can be improved via modifying the selected V2V mode to V2I mode, which can achieve a larger $C^P_{i,j}$ without impairing DENM and CAM transmissions. To be specific, for $V_{i,j}$, if modifying the transmission in $S_{i,m}$ from V2V mode to V2I mode, the impacts on following aspects are considered:

- $C^P_{i,j}$ – Owing to the modification, $S_{i,m}$ can be applied by $V_{i,j}$ for CPM transmission, and the $B_{i,m}$ is updated correspondingly. Hence, the $C^P_{i,j}$ is updated with the added $\left(A_{i,j,m}/B_{i,m}\right)$ RBs;
- $C^P_{i,k}, k \neq j$ – For other groups belonged to T_i segment, if $S_{i,m}$ is available for CPM transmissions, $C^P_{i,k}$ is reduced due to the larger $B_{i,m}$. Otherwise, $C^P_{i,k}$ is not changed;
- C^P_R – Since one more transmission is selected for V2I mode, more RBs are required for V2I DL transmissions. Thus, the C^P_R is reduced with the larger D_r.

If $T^P_{i,j}$ is larger than T^P_R, T^P can be reduced through adjusting the selected V2V mode to V2I mode for the group with the highest $T^P_{i,j}$. Although the initial RB allocation results for DENM and CAM transmissions are achieved in Subsection V-A, we still can adjust the RB allocation to minimize the CPM uploading interval, as given in Algorithm 1.

Algorithm 2 Resource Allocation for CPM

1 **Input:** Initial RB allocation results for DENM and CAM transmissions; sensing quality maps of SCVs;
2 **Output:** CP seed vehicle set, $\mathbb{V}^s$; required CPM period, T^P; V2I UL RB allocation for $\mathbb{V}^s$;
3 **Initialization**:
4 CP seed vehicle set, $\mathbb{V}^s = \{\}$;
5 Sensing error for each block, e_0; the overall error, E_0;
6 **Phase1**: Identify the groups supporting the CPM uploading:
7 With $R^P_{i,j} = 1$, run Algorithm 1 and obtain $C^P_{i,j}$;
8 Establish candidate CP seed vehicle set $\mathbb{V}^c$, consists of the SCVs in the groups with positive $C^P_{i,j}$;
9 **Phase2**: Select SCVs to reach the coverage rate threshold:
10 **while** *Coverage rate* $< C$ **do**
11   Find the SCV in $\mathbb{V}^c$ with the highest sensing gain;
12   Add the selected SCV to $\mathbb{V}^s$, and remove it from $\mathbb{V}^c$;
13   Update sensing errors for the newly sensed blocks;
14   Calculate the coverage rate and overall sensing error;
15 $R^P_{i,j} \leftarrow$ the number of CPM requests in each group $V_{i,j}$;
16 Run Algorithm 1 and obtain the required CPM period T^P;
17 Update the overall error as E_{T^P} by considering the additional error caused by the CPM update latency;
18 **Phase3**: Select SCVs to improve the sensing quality:
19 Let $E_{T^P-1} = E_0$;
20 **while** $E_{T^P} < E_{T^P-1}$ **do**
21   **while** *Required CPM period* $= T^P$ **do**
22   Repeat the steps from Line 11 to Line 14;
23   Update $R^P_{i,j}$;
24   Run Algorithm 1 and obtain the required CPM period;
25     $E_{T^P} \leftarrow$ the achieved minimal overall error with current CPM period T^P;
26     $T^P = T^P + 1$;
27 Find the optimal T^P with the minimal overall error and the corresponding $\mathbb{V}^s$;
28 **Phase4**: V2I UL RB allocation:
29 Allocate V2I UL RBs to each vehicle in $\mathbb{V}^s$, according to the remaining wireless resources in its belonging group.

The procedures of determining which vehicle groups require to be adjusted are given from Line 3 to Line 4, and the detailed procedures of RB allocation adjustment are given from Line 5 to Line 18. Specifically, the CPM uploading capacity is calculated for each potential adjustment in Line 8. Then for the cases with non-zero capacity, adjustment will be performed, as given from Line 9 to Line 14. The output of Algorithm 1 includes the updated RB allocation for DENM and CAM transmissions, the CPM period, $C^P_{i,j}$, and C^P_R, which will then be used to determine the CP seed vehicle selection.

In Fig. 6, an example of DENM, CAM, and CPM RB allocation for group $V_{1,1}$ is illustrated, where $R^P_{1,1} = 2$ and $T^P = 3$. To allocate the V2I UL RBs for CPM transmissions, the resource pool is extended to one CPM period (i.e., three CAM periods), and T^n_i denotes the T_i segment in the n-th CAM period. The RB allocation for DENM and CAM transmissions is repeated for each CAM period, obtained by running Algorithm 1. The RB allocation for CPM transmissions is designed based on the extended resource pool, such as the CP seed vehicles $V^3_{1,1}$ and $V^5_{1,1}$ shall transmit their CPM packets in T^2_1 and T^3_1 segments, respectively.

TABLE IV
SIMULATION PARAMETERS

Packet sizes (RB)	DENM / CAM	15	CPM UL / DL	50 / 250
Vehicular network parameters	Number of sub-channels	50	Number of sub-frames for each time segment	25
	Number of time segments	4	Number of DENMs per request	10
Communication model parameters	RSU communication range (m)	500	V2V communication range (m)	200
	Decoding threshold (dBm)	-75	Path-loss exponent, n_{NLOS}	2.69
	Receiver's antenna gain, G_r (dB)	3	Transmission power per RB, P_{TX} (dBm)	23
	Carrier frequency (GHz)	5.89	Critical distance, d_b (m)	100

2) Sensing Resource Allocation: The CP seed vehicles are selected to reach the coverage rate threshold and optimize the integrated sensing accuracy, represented by the overall sensing error within the area. To evaluate the overall sensing error, we divide the street area into small sensing blocks and calculate the sensing error of each block. Given an SCV, we can calculate its sensing error for the blocks, which is dependent on the sensing capability of the SCV. In addition, since a longer latency of sensing information update results in a larger sensing error, the CPM period T^P is also considered for sensing error calculation. For an SCV, its sensing error for a given block is

$$e = \begin{cases} w_d \cdot d + w_t \cdot T^P, & \text{if sensed,} \\ e_0, & \text{if not sensed,} \end{cases} \tag{7}$$

where w_d (w_t) is the unit sensing error caused by distance (the latency of CPM update), d is the distance between the block center and the SCV, and e_0 is the penalty error for not sensed blocks. Thus, for each SCV, its sensing quality map is built to represent its sensing performance, which is a matrix of e calculated for all blocks with $T^P = 0$.

The overall sensing error is obtained by accumulating the sensing error for all blocks. Based on the sensing quality maps of CP seed vehicles, the sensing error of each block is evaluated as the minimal e achieved by the selected SCVs. We propose an iterated method to select the CP seed vehicles and determine the required CPM period, as given in Algorithm 2. In each iteration, one SCV is added to the CP seed vehicle set, which is greedily selected based on the sensing gain. The sensing gain of one SCV is defined as the decrement of overall sensing error achieved by adding this SCV to the CP seed vehicle set. In **Phase1** of Algorithm 2, the RSU identifies the vehicle groups with adequate wireless resources for CPM uploading. Within the qualified groups, the SCVs are firstly selected to reach the sensing coverage threshold C in **Phase2** of Algorithm 2, in which the greedy CP seed vehicle selection is operated in Line 11 and the required CPM period is determined by running Algorithm 1 in Line 16. After reaching the coverage threshold, the SCVs are selected to improve the overall sensing accuracy as elaborated in **Phase3**. To minimize the sensing error caused by CPM update latency, the wireless resource allocation is adjusted (Algorithm 1) to minimize T^P. Hence, the selection of CP seed vehicles and optimization of wireless resource allocation are iteratively performed, as given in Line 22 and Line 24, respectively. Finally, V2I RBs are allocated to the selected CP seed vehicles to upload CPMs, as elaborated in **Phase4**.

C. V2I DL Resource Allocation

For the DENM and CAM transmitted under the V2I mode, S^D and S^A RBs are required for V2I DL transmissions, respectively. For CP services, the RSU broadcasts an integrated CPM packet in each CAM period, which requires S^{PD} RBs for V2I DL transmission. As shown in Fig. 4, for a packet transmitted via V2I mode, the RBs for DL transmission are allocated after the UL RB allocation. To minimize the packet transmission delay, DL RBs are allocated to achieve the minimal time gap away from the allocated UL RBs. Considering the transmission priority of different message types, the DL RB allocation performs following the allocation order of DENM, CAM, and CPM. In addition, considering the diversified receiver group size $M_{i,j}^m$, the transmitting vehicle with a larger $M_{i,j}^m$ has a higher priority on DL RB allocation. More specifically, DL RBs are firstly allocated for the vehicles with DENM requests, following the descending orders by $M_{i,j}^m$. Then, DL RBs are allocated for CAM transmissions in a similar way, followed by that for the CPM DL.

D. Resource Allocation Analysis for DENM and CAM

To analyze the resource allocation for DENM and CAM transmissions, we simulate the proposed SRA scheme based on the taxi GPS trace data set [30], including the vehicle ID, vehicle position, and the corresponding timestamp. We focus on a 800 m × 800 m square area, which covers two intersections. The DENM requests are randomly raised by vehicles, and a constant number of packets will be transmitted for each request. The numbers of required RBs for DENM, CAM, and CPM upload/download transmissions are given in Table IV. Moreover, the parameters of the vehicular network and the communication model [31] are given in Table IV.

Since the traffic density varies during peak and off-peak hours, the number of message transmission requests raised within each vehicle group changes accordingly. For one vehicle group, the numbers of RBs allocated for DENM and CAM transmissions are given in Fig. 7, with respect to the number of corresponding transmission requests. Both V2V and V2I modes are considered, and the sum of V2V and V2I UL RBs allocated for each message type is equal to its required number of RBs. Since the NLOS condition is severe at the intersection, V2I transmissions are required by most of the vehicles in the area, and thus the number of allocated V2I UL RBs, which is nearly proportional to the number of requests in Fig. 7(a). As each time segment consists of 25 sub-frames, the insufficient sub-frame condition happens when the overall number of requests becomes larger than 25,

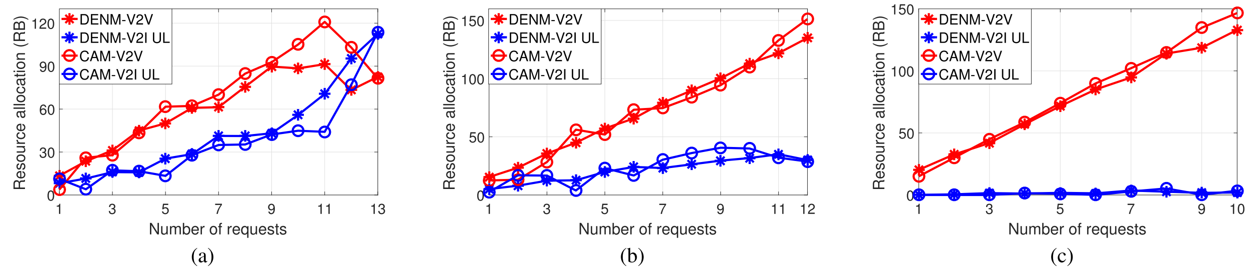

Fig. 7. Resource allocation results changing with the number of requests: a) at intersection; b) close to the intersection; c) away from the intersection.

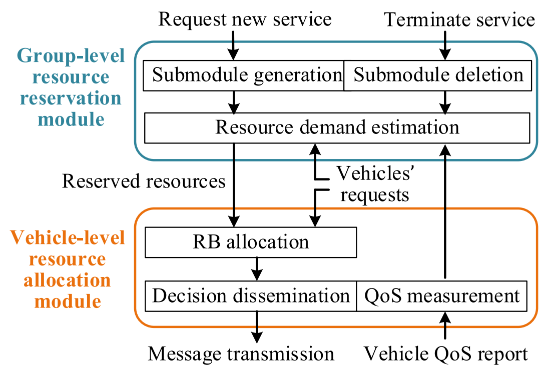

Fig. 8. Illustration of the resource reservation module and the resource allocation module.

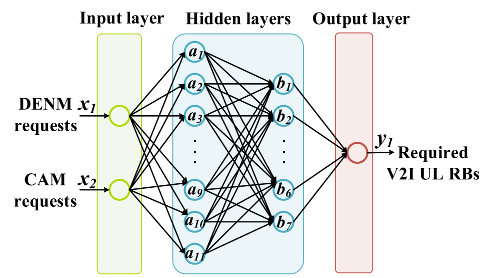

Fig. 9. BP network based resource demand estimation.

i.e., more V2I UL RBs are required at the last point in Fig. 7(a). If the group is close to the intersection, fewer vehicles are impacted by NLOS conditions, leading to smaller V2I resource requirements, as shown in Fig. 7(b). Considering the limited V2I UL resources, the number of V2I UL RBs becomes smaller slightly in Fig. 7(b) during the traffic peak hours, due to more V2I UL resource demands of the groups shown in Fig. 7(a). However, for the groups far from the intersection, most vehicles are assigned with V2V modes due to the good link quality, and hence the numbers of V2I RBs allocated for DENM and CAM transmissions become zero in Fig. 7(c). In addition to NLOS conditions, the differentiated priorities are considered for V2I resource allocation. Thus, when the V2I resources are scarce, more V2I RBs are allocated to the DENM transmission with a higher priority, as shown in Fig. 7(a).

VI. Resource Reservation and Resource Allocation Modules

As SRA scheme needs to sequentially make decisions for vehicles requesting different messages, TARA framework is proposed to enable parallel decision-making to improve the time efficiency. To make adaptive resource allocation decisions, a group-level resource reservation module and a vehicle-level resource allocation module are designed, as shown in Fig. 8. The resource reservation module distributes resources for different groups to satisfy their distinct QoS requirements. With the reserved resources, RBs are allocated to each vehicle by the resource allocation module.

A. Group-Level Resource Reservation Module

In the proposed resource allocation scheme for DENM and CAM transmissions introduced in Subsection V-A, the decision on NLOS-drive V2I mode selection is made iteratively for all the vehicles, which requires a large number of iterations, especially for the peak hours with high traffic density. To improve the efficiency of the resource allocation scheme, the numbers of V2I UL RBs allocated for DENM and CAM transmissions in each group are estimated by the resource reservation module, enabling the decoupling of the V2I mode selection among different groups.

As shown in Fig. 8, resource reservation module consists of three functionalities, two related to submodule formation (i.e., generation and deletion) and one for determining the amount of reserved resources for each message type (i.e., resource demand estimation). Since CAMs and CPMs are periodically broadcasted, the corresponding submodules are established as a default setting for each vehicle group by the resource reservation module. However, as the transmission of DENMs is event-triggered, the DENM submodule is established and deleted according to service requests. For each established submodule, the resource demand estimation function specifies the amount of reserved resources, based on the information of vehicles' requests. To be specific, for vehicle group $V_{i,j}$, the numbers of V2I UL RBs allocated to vehicles requesting for DENMs and CAMs are specified, denoted by $N_{i,j}^{D}$ and $N_{i,j}^{A}$, respectively.

The update is triggered by the detection of an unsatisfied submodule or a new submodule, as shown in Fig. 8. Here the unsatisfied message transmission is identified by QoS measurement results from the vehicle-level resource allocation module. If one submodule with insufficient resources is detected, the resource reservation module will first estimate the resources required by this submodule based on real-time requests. If the remaining resources are sufficient, the resource reservation result is only updated for the under-provisioning submodule. Otherwise, all the submodules require an update, including the redundant resource release

TABLE V
SENSOR PARAMETERS

Coverage range, R (m)	186
Sensing error per distance, w_d	0.05
Sensing evaluation block size (m)	3
Sensing coverage threshold, C	0.9
Additional sensing error per period, w_t (m)	1.4
Penalty sensing error, e_0 (m)	50

and resource supplement for the over-provisioning and under-provisioning submodules, respectively.

1) Resource Demand Estimation: In light of the analysis in Subsection V-D, the amount of allocated V2I UL RBs for DENM and CAM transmissions is closely correlated with the number of requests. Due to the priorities of different message types, the mapping relationships between requests and resources are diversified. On the other hand, the location of each vehicle group also determines its required amount of V2I UL resources, e.g., the vehicles approaching intersections are more likely to suffer from NLOS conditions and require V2I resources. In order to estimate the V2I UL RB demand, we model the mapping relationship for resource demand estimation. The severity degree of NLOS conditions in different street segments is difficult to be quantified, which is essential for modeling the mapping relationship mathematically. Without a precise mathematical model, the learning-based method, e.g. back propagation (BP) neural network [32], is a promising solution to this regression problem. Due to the multi-layer structure, the BP network has the capability to mimic complex nonlinear mapping relationship [33]. In addition, for unexpected inputs, the mechanism of backward propagation of errors enables weight adjustment to minimize the estimation error, which makes the method adaptive to dynamic vehicular networks. Hence, the BP network based resource demand estimation is trained for each vehicle group to estimate the required V2I RBs for DENM and CAM transmissions.

As shown in Fig. 9, for group $V_{i,j}$, a BP network is trained to learn the relationship between the input and the output, consisting of the input, hidden, and output layers. The numbers of received DENM and CAM requests are utilized as the input, and the output of the BP network is the allocated V2I UL RBs for DENM or CAM transmissions. To train the learning module, we run SRA scheme and record its V2I resource allocation results, to obtain the training dataset. One sample of input and output can be achieved during each CAM period. An advisable configuration is essential for the BP network to accurately estimate resource demand. We configure the neural network with different transfer functions and different numbers of nodes, and find the optimal configuration based on the experimental results. In doing so, the BP network is set with two hidden layers of the node number of 11 and 7 with the transfer functions of tansig and linear, respectively.

B. Vehicle-Level Resource Allocation Module

Based on the resource reservation result, the RB allocation function determines CP seed vehicle set and the V2V, V2I

Algorithm 3 RB Allocation for the DENM and CAM

1 **Input:** Vehicles' locations; DENM and CAM requests; resource reservation decisions, $N^D_{i,j}$ and $N^A_{i,j}$;
2 **Output:** V2V and V2I UL RB allocation decision;
3 Estimate the potential V2I gain for each vehicle, $G^m_{i,j}$;
4 **Phase1**: V2I mode selection:
5 **for** *Each group belonging to the RSU,* $V_{i,j}$ **do**
6 $V^D(V^A) \leftarrow$ the vehicles with DENM (CAM) requests;
7 **for** k=1:$\lfloor N^D_{i,j}/S^D \rfloor$ **do**
8 **while** V^D *is not empty* **do**
9 $\upsilon \leftarrow$ the vehicle with the highest $G^m_{i,j}$ in V^D;
10 Select the V2I mode for υ, remove υ from V^D;
11 **for** k=1:$\lfloor N^A_{i,j}/S^A \rfloor$ **do**
12 **while** V^A *is not empty* **do**
13 $\upsilon \leftarrow$ the vehicle with the highest $G^m_{i,j}$ in V^A;
14 Select the V2I mode for υ, remove υ from V^A;
15 $V^D_I(V^A_I) \leftarrow$ the vehicles requesting the DENM (CAM) transmission are assigned with V2I mode;
16 Select V2V mode for the requests without V2I mode;
17 **Phase2**: TDS identification:
18 **for** *Each time segment,* T_i **do**
19 Calculate the required number of TDSs, I_i;
20 **for** *Each group belonging to* T_i*,* $V_{i,j}$ **do**
21 Calculate $D_{i,j}$ and $I_{i,j}$;
22 **if** $I_i > \sum_{j=1}^{G_i} I_{i,j}$ **then**
23 Increase $I_{i,j}$ to satisfy $I_i = \sum_{j=1}^{G_i} I_{i,j}$ and modify the corresponding $D_{i,j}$;
24 $D_a(D_r) \leftarrow$ available (required) V2I DL RB number;
25 **while** $D_r > D_a$ **do**
26 **while** V^A_I *is not empty* **do**
27 $\upsilon \leftarrow$ the vehicle with the lowest $G^m_{i,j}$ in V^A_I;
28 Modify the transmission mode to V2V for υ;
29 Update V^A_I, D_a, and D_r (Line 18 to Line 24);
30 **while** V^D_I *is not empty* **do**
31 $\upsilon \leftarrow$ the vehicle with the lowest $G^m_{i,j}$ in V^D_I;
32 Modify the transmission mode to V2V for υ;
33 Update V^D_I, D_a, and D_r (Line 18 to Line 24);
34 **Phase3**: RB allocation:
35 **for** *Each time segment,* T_i **do**
36 Let $t_I = 1$, the first sub-frame available for V2I;
37 **for** *Each group belonging to* T_i*,* $V_{i,j}$ **do**
38 Assign the sub-frames $\left(t_I, t_I + I_{i,j} - 1\right)$ as TDSs;
39 Determine the sequential sub-frames, $\left(t^s_I, t^e_I\right)$, allocated for V2I transmission, where $t^s_I = t_I$;
40 **for** *The requests in* $V_{i,j}$ **do**
41 **if** *The V2I mode is selected for the request* **then**
42 **if** *There are unoccupied RBs in TDSs* **then**
43 Allocate the V2I RBs in TDSs;
44 **else**
45 Allocate the V2I RBs in the first unoccupied sub-frame within $\left(t_I + I_{i,j}, t^e_I\right)$;
46 **else**
47 Allocate the V2V RBs in the first unoccupied sub-frame out of $\left(t^s_I, t^e_I\right)$;
48 $t_I \leftarrow t^e_I + 1$;

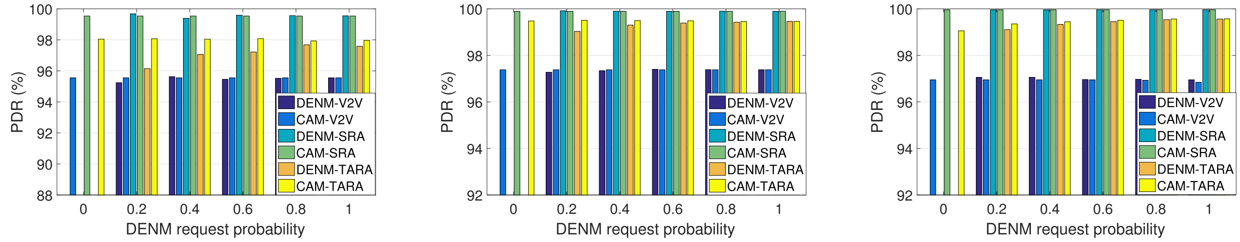

(a) (b) (c)

Fig. 10. PDR during: a) low traffic; b) medium traffic; c) high traffic.

UL, and V2I DL RBs allocated for each request. Then, vehicles receive the RB allocation decision and transmit the generated packets accordingly. At the end of each interval, the QoS measurement function measures the performance for message transmissions, according to the collected reports from vehicles. Comparing with the sequential decision-making in SRA scheme, the RB allocation decisions for DENM and CAM transmissions can be made in parallel in terms of groups and message types, as given in Algorithm 3. In each vehicle group, vehicles with higher $G_{i,j}^{m}$ are allocated with V2I RBs until the amount of V2I RBs reserved for this group is used up, as described by **Phase1**. Hence, the mode selection for DENMs and CAMs in different groups can be operated in parallel, which is more efficient than the method introduced in Subsection V-A. After assigning transmission modes for all vehicles, the number of required TDSs and requests transmitted in TDSs is calculated in **Phase2**. With the configuration of transmission mode and TDSs, the corresponding V2I or V2V RBs are allocated to each vehicle in **Phase3**. Based on the RB allocation result of DENMs and CAMs, the resource allocation for CPMs and the V2I DL RB allocation follow the procedures introduced in Subsection V-B and Subsection V-C, respectively.

VII. Numerical Results

In this section, we perform a trace-driven simulation of the proposed TARA framework to evaluate its performance, under the scenario introduced in Subsection V-D. Considering the impact of traffic, we perform the simulation during the hours of low (7:10 a.m.), medium (2:30 p.m.), and high (5:30 p.m.) traffic densities. We assume all vehicles are equipped with sensors, with the parameters given in Table V [34]. To show the flexibility of the proposed method, we evaluate the performance with varying probabilities of DENM requests.

A. Performance of DENM and CAM Transmissions

Both the reliability and delay are measured for DENM and CAM transmissions. Here, the reliability of each packet transmission is evaluated by the metric of PDR. As shown in Fig. 10, if all the transmissions are supported by V2V connections, nearly 96% of packets are successfully received during the low traffic hours, while a higher reliability is achieved during the medium and high traffic hours, owing to the decreased distance among vehicles. Since the packets can be relayed at the RSU, the packet loss resulting from NLOS conditions can be alleviated, and nearly 100% reliability is achieved by SRA scheme. Different from SRA, the resource allocation of TARA is based on the results of its resource reservation module. The reliability performance of 98% and 99% are respectively achieved for the low and high traffic scenarios. Notice that, for TARA results shown in Fig. 10, the reliability of DENM transmission degrades with a lower DENM request probability. This is because the resource reservation module tends to neglect the small number of DENM requests, and allocate the majority of V2I resources to CAM transmissions in this case.

To evaluate the delay of packet transmission, we measure the sub-frame gap between the allocated UL and DL RBs for each V2I mode transmission. Due to the simultaneous transmission and reception, the delay of V2V transmission is negligible. The average delay of packet transmissions with varying vehicle densities and DENM request probabilities is shown in Fig. 11. In the medium and high traffic scenarios, according to the priority order considered by the V2I DL RB allocation, a lower delay is achieved for the DENM transmission, comparing with that of the CAM. In the low traffic scenario, packets are mainly transmitted via V2V connections, and the high priority of DENM is not reflected by transmission delay results. Since the V2I DL RB allocation is implemented after the V2I UL RB allocation, if more V2I RBs are allocated for the UL transmission, the sub-frame gap between DL and UL can become larger due to the less options for DL RB allocation. Thus, the transmission delay increases with the vehicle density and DENM request probability, as shown in Fig. 11. Although the average delay achieved by TARA is longer than that of SRA, it still manages to be lower than 1.5 ms, 6 ms, and 8.5 ms during low, medium, and high traffic hours.

B. Performance of CPM Transmissions

For CP services, both the coverage rate (CP coverage) and the average sensing error (CP error) are evaluated as QoS metrics, under different traffic conditions, i.e., low (L), medium (M), and high (H) traffic densities. Since the area of interest is divided into blocks, the sensing error is measured for each block. In Fig. 12(a), the coverage refers to the proportion of sensed blocks to the amount of blocks within the area of interest, which is determined by the distribution of vehicles. Thus, with more vehicles on the street, the coverage rate becomes higher. The optimal CPM period is impacted by the vehicle density and the DENM probability. With a higher

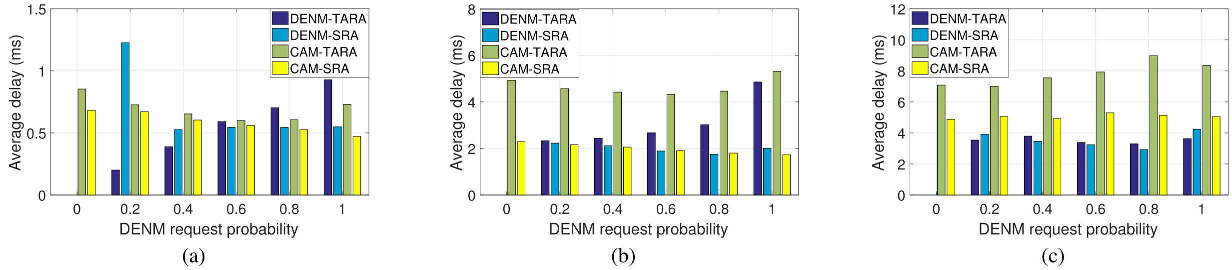

Fig. 11. Average transmission delay during: a) low traffic; b) medium traffic; c) high traffic.

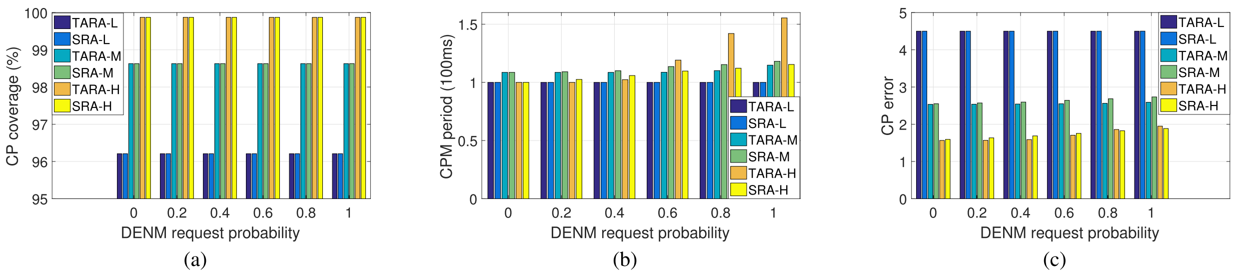

Fig. 12. Cooperative perception performance changing with DENM request probability: a) coverage rate; b) CPM period; c) average error.

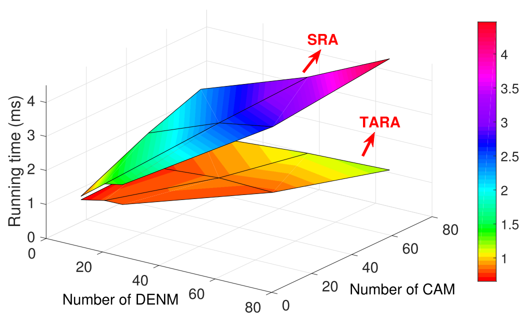

Fig. 13. Running time of the resource allocation schemes.

density of vehicles and a higher DENM request probability, more wireless resources are required to support DENM and CAM transmissions in each CAM period, which calls for a longer CPM period as shown in Fig. 12(b). On the other hand, with a higher density of vehicles, the sensing gain of selecting one more SCV decreases due to the more compact distribution of SCVs. Thus, for the condition with a high traffic density and a low DENM request probability, the optimal CPM period is 1, since the fact that the sensing gain achieved by selecting more SCVs is lower than the penalty of a longer CPM update latency. In Fig. 12(c), the average sensing error for each block is evaluated. Considering the penalty error for the area out of sensing coverage, the CP error with different traffic densities has a similar trend as that of the coverage rate. Meanwhile, a longer CPM uploading latency leads to a higher CP error, which can be observed through the similar increasing trends of the CPM period and the CP error.

C. Time Complexity of Resource Allocation Algorithms

To compare the time complexity of SRA and TARA, we evaluate the running time of their wireless resource allocation algorithms introduced in Subsection V-A and Algorithm 3, respectively. Both are run on an Intel i7-8750U CPU@2.2GHz. The running time is evaluated with varying traffic density and DENM request probabilities, i.e., the varying numbers of DENM and CAM transmissions handled by resource allocation algorithms. In Fig. 13, an almost linear increasing trend is observed for the average running time of SRA algorithm, while the increasing trend of TARA is negligible. Specifically, in the high traffic density scenario with the DENM probability of 0.9, the time consumed by SRA is three times longer than that of TARA. According to the evaluation results, TARA can make resource allocation decisions more efficiently than SRA, especially during the traffic peak hours with a large number of transmission requests. The simulation results indicate the low complexity of the proposed TARA framework in large-scale vehicular networks with satisfied delay and CP service requirements.

VIII. Conclusion and Future Work

In this paper, we have proposed TARA framework to support safety message transmissions in RSU-assisted urban vehicular networks. Specifically, TARA framework consists of a group-level resource reservation module and a vehicle-level resource allocation module to enable adaptive multi-dimensional resource allocation. For vehicles with DENM, CAM, or CPM requests, the multi-dimensional resource allocation decisions, including the V2I/V2V mode selection, RB allocation, and the CP seed vehicle selection, can be made to optimize the distinct performance metrics for different message types. The trace-driven simulation results have been provided to demonstrate the low latency and high PDR achieved for DENM and CAM transmissions, the high sensing quality achieved for CPM transmissions, and the robustness of the framework to adapt to dynamic traffic densities. Moreover, the proposed TARA framework can achieve real-time satisfying performance and be readily applied into large-scale vehicular networks. For the future work, considering the computation-intensive vehicular services, we will further investigate the joint allocation of computing, wireless, and sensing resources in vehicular networks for efficient service provisioning.

References

[1] J. Chen, H. Wu, F. Lyu, P. Yang, and X. Shen, "Multi-dimensional resource allocation for diverse safety message transmissions in vehicular networks," in *Proc. IEEE Int. Conf. Commun. (ICC)*, Jun. 2021, pp. 1–6.

[2] *Intelligent Transport Systems (ITS); Vehicular Communications; Basic Set of Applications; Part 2: Specification of Cooperative Awareness Basic Service*, document ETSI EN 302 637-2, Apr. 2019.

[3] F. Lyu *et al.*, "Towards rear-end collision avoidance: Adaptive beaconing for connected vehicles," *IEEE Trans. Intell. Transp. Syst.*, vol. 22, no. 2, pp. 1248–1263, Feb. 2021.

[4] *Intelligent Transport Systems (ITS); Vehicular Communications; Basic Set of Applications; Analysis of the Collective Perception Service (CPS)*, document ETSI TR 103 562 V2.1.1, Dec. 2019.

[5] *Intelligent Transport Systems (ITS); Vehicular Communications; Basic Set of Applications; Part 3: Specifications of Decentralized Environmental Notification Basic Service*, document ETSI EN 302 637-3, Aug. 2018.

[6] Y. Ni *et al.*, "Toward reliable and scalable internet of vehicles: Performance analysis and resource management," *Proc. IEEE*, vol. 108, no. 2, pp. 324–340, Feb. 2020.

[7] F. Lyu *et al.*, "Characterizing urban vehicle-to-vehicle communications for reliable safety applications," *IEEE Trans. Intell. Transp. Syst.*, vol. 21, no. 6, pp. 2586–2602, Jun. 2020.

[8] M. Noor-A-Rahim, G. G. M. N. Ali, Y. L. Guan, B. Ayalew, P. H. J. Chong, and D. Pesch, "Broadcast performance analysis and improvements of the LTE-V2 V autonomous mode at road intersection," *IEEE Trans. Veh. Technol.*, vol. 68, no. 10, pp. 9359–9369, Oct. 2019.

[9] H. Wu, F. Lyu, C. Zhou, J. Chen, L. Wang, and X. Shen, "Optimal UAV caching and trajectory in aerial-assisted vehicular networks: A learning-based approach," *IEEE J. Sel. Areas Commun.*, vol. 38, no. 12, pp. 2783–2797, Dec. 2020.

[10] J. Chen, H. Wu, P. Yang, F. Lyu, and X. Shen, "Cooperative edge caching with location-based and popular contents for vehicular networks," *IEEE Trans. Veh. Technol.*, vol. 69, no. 9, pp. 10291–10305, Sep. 2020.

[11] F. Lyu *et al.*, "MoMAC: Mobility-aware and collision-avoidance MAC for safety applications in VANETs," *IEEE Trans. Veh. Technol.*, vol. 67, no. 11, pp. 10590–10602, Nov. 2018.

[12] M. Zhang, G. G. M. N. Ali, P. H. J. Chong, B.-C. Seet, and A. Kumar, "A novel hybrid MAC protocol for basic safety message broadcasting in vehicular networks," *IEEE Trans. Intell. Transp. Syst.*, vol. 21, no. 10, pp. 4269–4282, Oct. 2020.

[13] S. M. O. Gani, Y. P. Fallah, G. Bansal, and T. Shimizu, "A study of the effectiveness of message content, length, and rate control for improving map accuracy in automated driving systems," *IEEE Trans. Intell. Transp. Syst.*, vol. 20, no. 2, pp. 405–420, Feb. 2019.

[14] H. P. Luong, M. Panda, H. L. Vu, and B. Q. Vo, "Beacon rate optimization for vehicular safety applications in highway scenarios," *IEEE Trans. Veh. Technol.*, vol. 67, no. 1, pp. 524–536, Jan. 2018.

[15] Y. Ni, J. He, L. Cai, J. Pan, and Y. Bo, "Joint roadside unit deployment and service task assignment for internet of Vehicles (IoV)," *IEEE Internet Things J.*, vol. 6, no. 2, pp. 3271–3283, Apr. 2019.

[16] Z. Ning *et al.*, "Intelligent edge computing in internet of vehicles: A joint computation offloading and caching solution," *IEEE Trans. Intell. Transp. Syst.*, vol. 22, no. 4, pp. 2212–2225, Apr. 2021.

[17] K. Xiong, S. Leng, J. Hu, X. Chen, and K. Yang, "Smart network slicing for vehicular fog-RANs," *IEEE Trans. Veh. Technol.*, vol. 68, no. 4, pp. 3075–3085, Apr. 2019.

[18] J. Mei, X. Wang, and K. Zheng, "Intelligent network slicing for V2X services toward 5G," *IEEE Netw.*, vol. 33, no. 6, pp. 196–204, Nov./Dec. 2019.

[19] S. Zhang, W. Quan, J. Li, W. Shi, P. Yang, and X. Shen, "Air-ground integrated vehicular network slicing with content pushing and caching," *IEEE J. Sel. Areas Commun.*, vol. 36, no. 9, pp. 2114–2127, Sep. 2018.

[20] G. Sun, G. O. Boateng, D. Ayepah-Mensah, G. Liu, and J. Wei, "Autonomous resource slicing for virtualized vehicular networks with D2D communications based on deep reinforcement learning," *IEEE Syst. J.*, vol. 14, no. 4, pp. 4694–4705, Dec. 2020.

[21] Y. Chen, Y. Wang, M. Liu, J. Zhang, and L. Jiao, "Network slicing enabled resource management for service-oriented ultra-reliable and low-latency vehicular networks," *IEEE Trans. Veh. Technol.*, vol. 69, no. 7, pp. 7847–7862, Jul. 2020.

[22] Y. Park, T. Kim, and D. Hong, "Resource size control for reliability improvement in cellular-based V2 V communication," *IEEE Trans. Veh. Technol.*, vol. 68, no. 1, pp. 379–392, Jan. 2019.

[23] L. F. Abanto-Leon, A. Koppelaar, C. B. Math, and S. Heemstra de Groot, "Impact of quantized side information on subchannel scheduling for cellular V2X," in *Proc. IEEE 87th Veh. Technol. Conf. (VTC Spring)*, Jun. 2018, pp. 1–5.

[24] L. F. Abanto-Leon, A. Koppelaar, and S. H. de Groot, "Subchannel allocation for vehicle-to-vehicle broadcast communications in mode-3," in *Proc. IEEE WCNC*, Apr. 2018, pp. 1–6.

[25] S. Park, B. Kim, H. Yoon, and S. Choi, "RA-eV2V: Relaying systems for LTE-V2V communications," *J. Commun. Netw.*, vol. 20, no. 4, pp. 396–405, Aug. 2018.

[26] T. Mangel, O. Klemp, and H. Hartenstein, "5.9 GHz inter-vehicle communication at intersections: A validated non-line-of-sight path-loss and fading model," *EURASIP J. Wireless Commun. Netw.*, vol. 2011, no. 1, p. 182, Nov. 2011.

[27] T. Mangel, F. Schweizer, T. Kosch, and H. Hartenstein, "Vehicular safety communication at intersections: Buildings, non-line-of-sight and representative scenarios," in *Proc. 8th Int. Conf. Wireless-Demand Netw. Syst. Services*, Jan. 2011, pp. 35–41.

[28] H. M. El-Sallabi, "Fast path loss prediction by using virtual source technique for urban microcells," in *Proc. IEEE 51st Veh. Technol. Conf. (VTC-Spring)*, May 2000, pp. 2183–2187.

[29] L. F. Abanto-Leon, A. Koppelaar, C. B. Math, and S. Heemstra de Groot, "System level simulation of scheduling schemes for C-V2X Mode-3," 2018, *arXiv:1807.04822*.

[30] *Didi Chuxing GAIA Initiative*. Accessed: Oct. 2019. [Online]. Available: https://gaia.didichuxing.com/

[31] *Study on LTE-Based V2X Services*, 3GPP, document TR 36.885 V14.0.0,Jul. 2016.

[32] L. Xu, J. Wang, H. Wang, T. A. Gulliver, and K. N. Le, "BP neural network-based ABEP performance prediction for mobile Internet of Things communication systems," *Neural Comput. Appl.*, vol. 32, pp. 16025–16041, Dec. 2019.

[33] L. Zhang, F. Wang, T. Sun, and B. Xu, "A constrained optimization method based on BP neural network," *Neural Comput. Appl.*, vol. 29, no. 2, pp. 413–421, Jan. 2018.

[34] Y. Wu, Y. Wang, W. Hu, X. Zhang, and G. Cao, "Resource-aware photo crowdsourcing through disruption tolerant networks," in *Proc. IEEE 36th Int. Conf. Distrib. Comput. Syst. (ICDCS)*, Jun. 2016, pp. 374–383.

Jiayin Chen (Member, IEEE) received the B.E. and M.S. degrees from the School of Electronics and Information Engineering, Harbin Institute of Technology, Harbin, China, in 2014 and 2016, respectively, and the Ph.D. degree from the University of Waterloo, ON, Canada, in 2021. She is currently a Post-Doctoral Research Fellow at The University of British Columbia, BC, Canada. Her research interests are in the area of vehicular networks and machine learning, with current focus on intelligent transport systems and big data.

Huaqing Wu (Member, IEEE) received the B.E. and M.E. degrees from the Beijing University of Posts and Telecommunications, Beijing, China, in 2014 and 2017, respectively, and the Ph.D. degree from the University of Waterloo, ON, Canada, in 2021. She is currently a Post-Doctoral Research Fellow at McMaster University, ON. Her current research interests include vehicular networks with emphasis on edge caching, wireless resource management, space-air-ground integrated networks, and application of artificial intelligence (AI) for wireless networks. She received the Best Paper Award at IEEE GLOBECOM 2018. She received the prestigious Natural Sciences and Engineering Research Council of Canada (NSERC) Postdoctoral Fellowship Award in 2021.

Feng Lyu (Member, IEEE) received the B.S. degree in software engineering from Central South University, Changsha, China, in 2013, and the Ph.D. degree from the Department of Computer Science and Engineering, Shanghai Jiao Tong University, Shanghai, China, in 2018. From October 2016 to October 2017 and from September 2018 to December 2019, he worked as a Post-Doctoral Fellow and a Visiting Ph.D. Student with the BBCR Group, Department of Electrical and Computer Engineering, University of Waterloo, Canada. He is currently a Professor with the School of Computer Science and Engineering, Central South University. His research interests include vehicular networks, beyond 5G networks, big data measurement and application design, and cloud/edge computing. He served as a TPC member for many international conferences. He is a member of the IEEE Computer Society, Communication Society, and Vehicular Technology Society. He was a recipient of the Best Paper Award of IEEE ICC 2019. He serves as an Associate Editor for IEEE SYSTEMS JOURNAL and a Leading Guest Editor for *Peer-to-Peer Networking and Applications*.

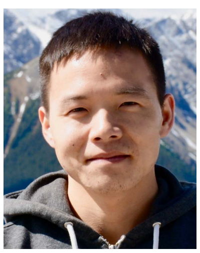

Peng Yang (Member, IEEE) received the B.E. degree in communication engineering and the Ph.D. degree in information and communication engineering from the Huazhong University of Science and Technology (HUST), Wuhan, China, in 2013 and 2018, respectively. He was a Visiting Ph.D. Student with the Department of Electrical and Computer Engineering, University of Waterloo, Canada, from September 2015 to September 2017, and a Post-Doctoral Fellow from September 2018 to December 2019. Since January 2020, he has been a Faculty Member with the School of Electronic Information and Communications, HUST. His current research focuses on next-generation networking, mobile edge computing, video streaming, and analytics.

Qihao Li (Member, IEEE) received the M.Sc. degree in information and communication technology from the University of Agder, Norway, in 2014, and the Ph.D. degree from the University of Oslo, Norway, in 2019. Since 2019, he has been a Post-Doctoral Fellow with the Department of Electrical and Computer Engineering, University of Waterloo. His current research interests include industrial wireless sensor networks, optimal control and optimization, wireless network security, and localization. He served or serving as a member for Technical Program Committee for IEEE GLOBECOM (2017–2021), IEEE ICC (2018–2021), IEEE CIC ICCC (2017–2021), and EuCAP (2019).

Xuemin (Sherman) Shen (Fellow, IEEE) received the Ph.D. degree in electrical engineering from Rutgers University, New Brunswick, NJ, USA, in 1990.

He is currently a University Professor with the Department of Electrical and Computer Engineering, University of Waterloo, Canada. His research focuses on network resource management, wireless network security, the Internet of Things, 5G and beyond, and vehicular networks. He is a Registered Professional Engineer of ON, Canada. He is an Engineering Institute of Canada Fellow, a Canadian Academy of Engineering Fellow, a Royal Society of Canada Fellow, and a Chinese Academy of Engineering Foreign Member. He was the Vice President for Technical and Educational Activities, the Vice President for Publications, a Member-at-Large on the Board of Governors, the Chair of the Distinguished Lecturer Selection Committee, and a member of IEEE Fellow Selection Committee of the ComSoc. He is the President Elect of the IEEE ComSoc. He received the Canadian Award for Telecommunications Research from the Canadian Society of Information Theory (CSIT) in 2021, the R. A. Fessenden Award from IEEE, Canada, in 2019, the Award of Merit from the Federation of Chinese Canadian Professionals (Ontario) in 2019, the James Evans Avant Garde Award from the IEEE Vehicular Technology Society in 2018, the Joseph LoCicero Award in 2015, the Education Award from the IEEE Communications Society (ComSoc) in 2017, and the Technical Recognition Award from Wireless Communications Technical Committee (2019) and AHSN Technical Committee (2013). He has received the Excellent Graduate Supervision Award from the University of Waterloo in 2006 and the Premier's Research Excellence Award (PREA) from the Province of Ontario, Canada, in 2003. He served as the Technical Program Committee Chair/Co-Chair for IEEE GLOBECOM'16, IEEE Infocom'14, IEEE VTC'10 Fall, and IEEE GLOBECOM'07. He served as the Chair for the IEEE ComSoc Technical Committee on Wireless Communications. He served as the Editor-in-Chief for the IEEE INTERNET OF THINGS JOURNAL, *IEEE Network*, and *IET Communications*. He is a Distinguished Lecturer of the IEEE Vehicular Technology Society and Communications Society.